Title: Ara h 1 protein–antibody dissociation study: evidence for binding inhomogeneities on a molecular scale

Author: E. Pérez-Ruiz D. Spasic A. Gils L.J. van IJzendoorn M.W.J. Prins J. Lammertyn

PII: S1871-6784(15)00021-7
DOI: http://dx.doi.org/doi:10.1016/j.nbt.2015.02.004
Reference: NBT 759

To appear in:

Received date: 1-11-2014
Revised date: 19-1-2015
Accepted date: 7-2-2015

Please cite this article as: Pérez-Ruiz, E., Spasic, D., Gils, A., van IJzendoorn, L.J., Prins, M.W.J., Lammertyn, J.,Ara h 1 proteinndashantibody dissociation study: evidence for binding inhomogeneities on a molecular scale, *New Biotechnology* (2015), http://dx.doi.org/10.1016/j.nbt.2015.02.004

Ara h 1 protein − antibody dissociation study: evidence for binding inhomogeneities on a molecular scale

E. Pérez-Ruiz[1], D. Spasic[1], A. Gils[2], L.J van IJzendoorn[3,5], M.W.J. Prins[3,4,5] and J. Lammertyn[1,†]

[1]Department of Biosystems - MeBioS, KU Leuven, Leuven, Belgium

[2]Department of Pharmaceutical & Pharmacological Sciences, Laboratory for Therapeutic and Diagnostic Antibodies, KU Leuven, Leuven, Belgium

[3]Department of Applied Physics, Eindhoven University of Technology, Eindhoven, The Netherlands

[4]Department of Biomedical Engineering, Eindhoven University of Technology, Eindhoven, The Netherlands

[5]Institute for Complex Molecular Systems, Eindhoven University of Technology, Eindhoven, The Netherlands

†Corresponding Author:

Postal address: Willem de Croylaan 42 - box 2428, 3001, Leuven

e-mail: jeroen.lammertyn@biw.kuleuven.be

telephone: +32 16 32 14 59

fax: +32 16 322955

Abstract

The characterisation of biomolecular interactions is essential when designing novel biosensors, since the interaction between the bioreceptor and the ligand determines important biosensing parameters such as sensitivity and selectivity. In this paper we study the interaction of the trimeric Ara h 1 protein with a monoclonal anti-Ara h 1 antibody by means of magnetic force-induced dissociation. The proteins were bound to magnetic particles and polystyrene surfaces by EDC/NHS reaction chemistry and by physisorption, respectively. Two different molecular configurations have been investigated, with either the Ara h 1 protein on the particles or the Ara h 1 protein on the polystyrene surface. A model with a Gaussian distribution of energy barriers for dissociation gives an adequate description for the measured multi-exponential decays. We hypothesise that distributions of molecular orientations as well as experimentally-induced variations may underlay the observed distributions. The two molecular configurations show a different peak value of the energy distribution. Similarly, SPR experiments for two distinct configurations (either Ara h 1 protein on the surface, or anti-Ara h 1 antibody on the surface) also show clear differences in dissociation behavior. We hypothesise that the multivalency of the involved molecules leads to different modes of binding. The results of this work highlight the importance of molecular inhomogeneities when studying the interaction processes of biomolecular complexes.

Key words: Force-induced dissociation; Magnetic Tweezers; SPR; Dissociation rate constant; Protein-antibody interaction; Ara h 1

1. Introduction

Biosensors exploit the specificity and strength of biomolecular interactions for the sensitive detection of analytes. Since their performance is determined by the nature and affinity of these interactions, it is important to properly characterise them. Dynamic force spectroscopy (DFS) techniques [1] have been exploited extensively for investigating biomolecular interactions and for studying the dissociation properties of molecular bonds. These techniques rely on the application of a force to a molecular bond and on the measurement of its force-induced dissociation characteristics. From this type of experiment, parameters such as the dissociation rate constant and the position of the energy barrier along the reaction coordinate (x_β) can be calculated. Many different techniques have been used for DFS, e.g. atomic force microscopy (AFM) [2,3], biomembrane force probes (BFP) [4,5], microneedles [6], optical tweezers (OT) [7] and nanopores [8]. These techniques follow only one interaction at a time and have proved to be powerful for investigating single molecule mechanics, as well as interactions between single molecules. However, it is difficult and time-consuming to achieve statistically relevant results [9]. Magnetic tweezers (MT) have appeared as an interesting alternative to measure multiple molecular interactions in parallel, as previously shown by ourselves and others [10–12]. In this approach, magnets generate a magnetic field gradient which allows application of the same force to many particles simultaneously, thus increasing the throughput [13,14].

When MT are applied in force-induced dissociation studies, the Bell and Evans model [1,15] is typically used to extract parameters from the observed dissociation curves. This model is based on the assumption that a single type of bond results in a single dissociation rate constant, caused by a single energy barrier for dissociation being present in the system.

Depending on the different populations of bound particles in the sample, a mono- or a multicomponent dissociation pattern is displayed in the dissociation curves. Therefore, the model can be extended to include these multiple populations, each with their own dissociation rate constant: multi-exponential Bell and Evans model [11,12]. This interpretation relies on the presence of a well-defined energy barrier along the reaction coordinate, but in practice dissociation of many ligand-receptor pairs from functionalised biosensor surfaces can show a more heterogeneous character. Recently, a model was proposed which assumes a distribution of energy barriers for particles bound to a surface by a ligand-receptor interaction [16]. This model provides information on the distribution of energy barriers in a multi-particle dissociation experiment and thus on the inhomogeneity of the prepared surface, which should be applicable to both specific and nonspecific interactions.

In this work we study the molecular interaction between an antibody─protein pair with magnetic force-induced dissociation experiments and interpret the data with both the classic multi-exponential Bell and Evans model (MBE) and the recently proposed model that assumes a distribution of energy barriers (DEB). Two different molecular configurations are studied. In the first one the protein is immobilised on a polystyrene substrate and the antibody is coupled to the surface of magnetic particles. In the second configuration, the arrangement of the biomolecules is inverted and therefore the antibody is immobilised on the substrate, while the protein is on the magnetic particles surface. Additionally, dissociation measurements with surface plasmon resonance (SPR) [17] are performed also for two molecular configurations, namely with the antibody coupled to the sensor chip surface and protein free in solution and, vice versa, with the protein on the chip surface and the antibody free in solution. The dissociation parameters obtained with the two different experimental techniques for the two biomolecular configurations are discussed in order to explore whether

the binding affinity of the studied antibody-protein complex is affected by how molecules are coupled to substrates.

The complex formed between the peanut allergen, Ara h 1 protein, and its monoclonal antibody, anti-Ara h 1, was chosen as a model system. Peanut allergy is one of the most severe and persistent hypersensitivity reactions to foods [18,19]. Since labeling legislation is becoming stricter [20,21], the need for sensitive biosensors that can detect low quantities of peanut allergens is also increasing. To date, several immunoassay techniques have been described in the literature [22–26]. In all of them the specificity and sensitivity of the assays were determined by the affinity and strength of the interaction between anti-Ara h 1 antibodies and Ara h 1 protein. Because similar types of interactions are found in many immunoassay-based biosensors, the conclusions of this work reach beyond the specific model system studied here.

2. Material and Methods

2.1 Reagents and Biomolecules

All buffer reagents were supplied by Sigma-Aldrich (The Netherlands). All solutions were prepared using deionised water purified with a Milli-Q Simplicity 185 system (Millipore). Natural Ara h 1, extracted from light roasted peanut flour (purity < 95%), and monoclonal anti-Ara h 1 antibody 2C12 were purchased from Indoor Biotechnologies Limited (UK). Carboxyl acid-coated superparamagnetic particles of 2.8 μm diameter (Dynabeads^{TM} M-270 Carboxylic Acid) were acquired from Thermo Fisher Scientific (Norway).

2.2 Functionalisation of superparamagnetic particles and polystyrene surfaces

Both the Ara h 1 protein and the anti-Ara h 1 antibody were coupled to 2.8 μm diameter carboxyl coated Dynabeads™ M-270 by a carbodiimide reaction [27]. The carboxyl groups were first activated for 20 min with 0.4 M 1-Ethyl-3-(3 dimethylaminopropyl)carbodiimide (EDC) and 0.5 M N-hydroxysuccinimide (NHS) in a 25 mM 2-(N-morpholino)ethanesulfonic acid (MES) buffer (pH 5). After washing the particles with MES buffer, they were resuspended in a solution of MES buffer containing either 3 μg/μL Ara h 1 antibody or 3 μg/μL Ara h 1 protein. Afterwards the functionalised particles were incubated during 30 min with 50 mM cold ethanolamine, followed by washing and storage in 150 mM phosphate buffered saline (PBS) solution (pH 7.4) containing 0.5% BSA and 0.01% Tween 20.

Polystyrene substrates 22×22 mm in size (Agar Scientific, U.K.) were cleaned with a nitrogen gas flow. Afterward an open cell of 9 mm in diameter and 0.12 mm in depth was created on a polystyrene surface using a double-sided adhesive cell-dot (Secure-Seal imaging spacer, Sigma-Aldrich, The Netherlands). The two different biomolecules (Ara h 1 and anti-Ara h 1 antibody) were immobilised by physical adsorption on the polystyrene surface enclosed within the cell. For that purpose, a 150 μL droplet of the respective biomolecule solution prepared in 150 mM PBS buffer was incubated during 1 h at room temperature inside the cell area. Finally, all modified polystyrene surfaces were blocked with 1% bovine serum albumin (BSA) solution also prepared in 150 mM PBS buffer.

2.3 Magnetic force-induced dissociation experiments

The functionalised magnetic particles were diluted 15 times from stock concentration (30 mg/mL) for further application on the modified polystyrene surfaces. The cell was closed with a glass microscope coverslip, 15×15 mm in size, and the particles were incubated for 3 min on the treated surface. After this incubation, the samples were inverted in order to remove

unbound particles from the surface by gravitational forces. Subsequently, magnetic pulling forces of different magnitudes in the picoNewton range were applied on these samples.

The magnetic force-induced dissociation technology setup consists of three different parts: (1) a microscope-camera system for imaging and recording, (2) a sample holder that supports the fluid cell in which the force-induced dissociation experiments take place and (3) an electromagnet to apply a constant mechanical pulling force. This technology was previously described in detail in Jacob *et al*. [11] and Pérez-Ruiz *et al*. [12]. In short, the fluid cell with functionalised magnetic particles bound to the top polystyrene surface, was placed on the sample holder lying on top of an electromagnet with a tapered pole-tip of 1 mm radius. The magnetic field was controlled by the current going through the coil and a water pump was used as a cooling system. This enabled continuous operation below 45°C. Moreover, to reduce the rise-time of the current and to allow the application of time-dependent currents for demagnetisation of the core, a push-pull current controller was developed. The magnet core was demagnetised after every force application.

The particles bound to the polystyrene surface were tracked with a Leica DM6000 microscope and images were acquired at 30 Hz frame rate by a RedLake MotionPro HS-3 speed camera triggered to the electromagnet through a function generator (Agilent, 33250A). The first frame at t=0 captured the total number of particles bound on the surface before the application of the force. The detachment of the particles was observed starting from the second movie frame. By counting the particles that were attached to the polystyrene surface through consecutive image frames, the dissociation curve for each applied force was obtained. The counting was done by a home-written MatLab (The MathWorks Inc., US) program, which gave the number of particles that were present in each frame as an output. The fitting of the dissociation curves was performed using Origin® software (The OriginLab Corporation, US).

2.4 Multi-exponential Bell and Evans model (MBE)

The dissociation rate constant of a molecular bond at zero force, $k_{off}(0)$ (s^{-1}), can be related to the energy barrier of the transition state, E_b, according to the Bell and Evans model [1,15]:

$$k_{off}(0)=\omega_0 \exp\left(-\frac{E_b}{k_B T}\right) \quad (1)$$

in which ω_0 is the attempt frequency that depends on the molecular details of the interaction, k_B is the Boltzmann constant and T is the temperature. When a transitional pulling force, F (pN), is applied, the energy needed to overcome the transition state is lowered by the work done along the reaction coordinate upon dissociation: W= -Fx_β, where x_β (nm) is the distance between the minimum and the maximum of the energy barrier, i.e. the distance by which the molecules must be separated in order to break the bond between them. Therefore the dissociation rate of a molecular bond changes exponentially with the applied force:

$$k_{off}(F)=\omega_0 \exp\left(-\frac{E_b - F\cdot x_\beta}{k_B T}\right)=k_{off}(0) \exp\left(\frac{F\cdot x_\beta}{k_B T}\right) \quad (2)$$

Thus, by varying the force applied to break the bond between ligand and receptor, it is possible to extrapolate the dissociation rate constant to zero force, $k_{off}(0)$, as the logarithm of $k_{off}(F)$ increases linearly with the increase in force, F:

$$\ln k_{off}(F)=\ln k_{off}(0)+\frac{F\cdot x_\beta}{k_B T} \quad (3)$$

By fitting this expression to force-dependent dissociation data, the transition-state distance, x_β, can be obtained. If the pulling force is applied for a time, t (s), the fraction of remaining bonds can be described as:

$$\frac{N}{N_0}=\exp\left(-k_{off}(F)\cdot t\right) \quad (4)$$

with N_0 the total number of bonds at t= 0 and N the total number of bonds present in the system. Depending on the different populations of bound particles in the samples (e.g. specifically vs. non-specifically bound particles, or single-bond vs. multiple-bond particles), typically a multicomponent dissociation pattern is displayed in the dissociation curves. Accordingly, the data analysis is performed with a multi-exponential Bell and Evans model (MBE).

2.5 Distributed Energy Barrier model (DEB)

The DEB model was recently described by Kemper et al. [16]. It is an extended interpretation of the Bell and Evans model that accounts for inhomogeneities present in the studied ligand-receptor interactions, represented as a distribution of energy barriers. Since this distribution is generally expected to be continuous, it is described by a Gaussian distribution around the central energy barrier value, $E_{0,}$ with a standard deviation, σ:

$$f(E_b) = \frac{1}{\sigma\sqrt{2\pi}} \exp\left(-\frac{(E_b - E_0)^2}{2\sigma^2}\right) \quad (5)$$

In this case the number of particles that remain on the surface after applying a magnetic force during a time, t (s), is given by a weighted integral over the distribution of energy barriers:

$$\frac{N}{N_0} = \int_{-\infty}^{\infty} \exp\left(-t\omega_0 \exp\left[-\frac{E_b - F \cdot x_\beta}{k_B T}\right]\right) \cdot \frac{1}{\sigma\sqrt{2\pi}} \exp\left(-\frac{(E_b - E_0)^2}{2\sigma^2}\right) dE_b \quad (6)$$

with N_0 the total number of bonds at t= 0 for all possible energy barriers and N the total number of bonds present in the system. Dissociation curves fitted by this equation deliver values for both E_0 and σ, provided that values are available for ω_0 and x_β.

2.6 Surface Plasmon Resonance (SPR) experiments

SPR experiments were conducted on a Biacore™ 3000 analytical system (Biacore AB, Sweden) using Biacore™ sensor chips CM5 consisting of a gold-coated glass slide modified with a carboxymethyl dextran layer. The flow cells of the chip were first activated by

injecting a 35 µL mixture of 50 mM NHS: 200 mM EDC. Subsequently, a solution containing either 1 µg/mL of anti-Ara h 1 antibody or 1 µg/mL of Ara h 1 protein in sodium acetate pH 4.5 was injected. The immobilisation levels reached were 84 and 129 resonance units (RU), respectively. Finally 35 µL of ethanolamine was injected to block any remaining activated ester groups, followed by 10 µL of 10 mM glycine pH 1.5 to remove any unbound antibody from the sensor surface. Flow cell 1, which was NHS/EDC activated and subsequently ethanolamine deactivated, was used as a reference channel in all experiments. Both Ara h 1 protein and anti-Ara h 1 antibody solutions of different concentrations ranging from 125 to 1000 nM were prepared in HBS-EP buffer (10 mM HEPES pH 7.4, 450 mM NaCl, 3 mM EDTA, 0.005% (v/v) polysorbate 20). Subsequently, either the Ara h 1 protein solutions or the anti- Ara h 1 antibody solutions were injected at a flow rate of 30 µL/min. Association time was 8 mins and dissociation time was 10 mins. The 10 mM glycine solution was also used to regenerate the chip surface between consecutive analyses in both cases. Temperature was fixed at 25°C during all experiments. A sensorgram corrected for both the reference channel (flow cell 1) and the response of the blank injection [28] was obtained for each concentration. To determine the binding kinetics, all data were analyzed using the Biacore™ evaluation software 4.1 (Biacore AB, Sweden).

3. Results and discussion

3.1 Establishing the experimental conditions for the magnetic force-induced dissociation experiments

The complex formed between the peanut allergen Ara h 1 protein and its monoclonal antibody was chosen as a model system to study the dissociation of protein-antibody complexes. As explained in section 2.3, superparamagnetic particles were functionalised with the anti-Ara h 1 antibody and incubated with polystyrene surfaces functionalised with Ara h 1 protein. To be able to extract dissociation rate constant values, it is important to average the individual

behavior of many single-molecule dissociation processes [10–12]. Therefore, the concentration of Ara h 1 protein to be immobilised on the polystyrene surface was optimised toward a concentration allowing for numerous single binding events on the surface, but avoiding that multiple bonds would dominantly be formed between the individual anti-Ara h 1 coated particles and the surface. Previously, other protein-receptor pairs [11] yielded consistent dissociation rates when the proteins were immobilised on the surface in a concentration range 0.01 - 1 nM, which indicated that single bonds were being measured. Consequently, we immobilised Ara h 1 protein on the polystyrene slides within the same concentration range (**Figure 1C-E**).

A concentration of 1 nM of Ara h 1 protein was chosen as the optimal concentration for the dissociation experiments since the number of particles immobilised on the surface was sufficiently high for statistical analysis, but still within the range where single bonds are being measured. To perform a negative control, magnetic particles functionalised with anti-Ara h 1 antibody were incubated with a polystyrene slide coated only with a solution containing 1% BSA. As it can be seen from Figure 1A, binding of functionalised magnetic particles to this surface is only ~2% of the binding to a 1 nM Ara h 1 protein coated surface. This suggests that there were barely nonspecific adsorptions of magnetic particles and that the binding to the 1 nM-prepared surface happened primarily through the specific interactions between antibody and its ligand.

3.2 Analysis of the dissociation of Ara h 1─anti-Ara h 1 complex with the Bell and Evans model (MBE)

Subsequently, magnetic force-induced dissociation experiments were performed by applying different magnetic pulling forces, ranging from 10 to 40 pN, to the particles bound on the

functionalised polystyrene surfaces. For each applied force, two different samples were measured resulting in two dissociation curves. The fraction of particles remaining after pulling during time t is plotted on a semi logarithmic scale in **Figure 2** and clearly shows that dissociation kinetics cannot be described by a single energy barrier. The Bell and Evans model can nevertheless be used to interpret the observed data assuming several fractions [11]: e.g. a weakly bound fraction of particles with a fast dissociation rate and a stronger bound fraction with slower dissociation rate. Since a passive adsorption of antibodies on hydrophobic surfaces leads to a mixture of orientations [29,30], the fast dissociation rate might be attributed to non-specific interactions between anti-Ara h 1 antibody and Ara h 1 protein. The second component, a stronger bound fraction with a slow dissociation rate, then originates from the specific interaction between both biomolecules when they are favorably oriented. This hypothesis is supported by the fact that when a control protein (human immunoglobulin E, IgE) was adsorbed on a polystyrene slide, magnetic particles with anti-Ara h 1 antibody also bound to this surface. However, upon incubation under the same conditions, the IgE surface captured only ~15% of the particles bound when the surface was coated with a 1 nM Ara h 1 protein solution (Figure 1B). This shows that a small fraction of antibody-modified particles interacts in a non-specific way with passively-adsorbed proteins on the surface, which also would apply in Ara h 1–anti-Ara h 1 antibody experiments.

Based on these two fractions of bound particles, a bi-exponential model with three independent parameters can be proposed for fitting the dissociation curves:

$$N = N_s \exp\left(-k_{off}^{s} \cdot t\right) + \left(1 - N_s\right) \exp\left(-k_{off}^{ns} \cdot t\right) \quad (7)$$

Using this equation, both dissociation rates for the non-specific (k_{off}^{ns}) and for the specific interactions (k_{off}^{s}) between Ara h 1 and anti-Ara h 1 antibody, as well as the population of particles specifically bound in each experiment at time t = 0, can be obtained.

Hence, the obtained dissociation curves were fitted by Equation 4 (Figure 2) and the extracted dissociation rates were plotted as a function of the applied force on a logarithmic scale according to Equation 3 (**Figure 3A**). Using the biexponential model, the obtained rate constant for dissociation at zero force for the specific binding, k_{off}^{s}, between Ara h 1 protein and anti-Ara h 1 antibody is found to be 2.2 ± 0.5 $\times 10^{-3}$ s^{-1}, with a x_β value of 1.6 ± 0.3 Å.

One of the assumptions underlying the employed biexponential model is that two fractions of particles are present at the surface. The fraction of specifically bound particles is a free parameter in the fitting procedure and should be independent of the applied force. However, when the fractions corresponding to each dissociation component were plotted versus the applied force (Figure 3B), they showed a significant dependency on the force. This invalidates the use of the MBE model with two fractions, since, obviously, more than two exponentials are required to explain the data. Previously, Jacob et al. [11] incorporated the existence of multiple bonds in the data analysis by adding a third exponential to the fitting equation, representing a strongly bound fraction of particles:

$$N = N_s \exp\left(-k_{off}^{s} \cdot t\right) + N_{ns} \exp\left(-k_{off}^{ns} \cdot t\right) + \left(1 - N_s - N_{ns}\right) \exp\left(-k_{off}^{m} \cdot t\right) \quad (8)$$

In order to investigate whether multiple bonds are also present in the Ara h 1–anti-Ara h 1 system, the obtained dissociation curves were also fitted by the triple-exponential model (Equation 8) (Figure S1). With this model, the fraction of particles corresponding to each of the dissociation components still depends on the applied force (Figure S2). These results invalidate the use of the MBE model to explain the dissociation data of the studied Ara h 1–anti-Ara h 1 antibody system.

3.3 Analysis of the dissociation of Ara h 1─anti-Ara h 1 complex with DEB model

The Bell and Evans model has been applied in many particle-based magnetic force-induced dissociation assays [10–12] based on the assumption that a unique energy barrier can be defined for a specific bond, in spite of the heterogeneity that is typically found in the molecular surfaces used in these experiments. This heterogeneity has been incorporated in the DEB model described by Kemper et al. [16], which assumes a distribution of energy barriers for dissociation instead of a single energy barrier. A mechanism that can generate a distribution is that biomolecules are coupled to a surface in different orientations, causing differences in reaction coordinates upon dissociation by a uniaxial external force. The DEB model is applicable to both specific and nonspecific interactions and typically shows a wider distribution for the first ones [16]. In the experiments described here, the anti-Ara h 1 antibody and the Ara h 1 protein molecules were either physically adsorbed on a polystyrene surface or coupled through EDC/NHS chemistry to magnetic particles. Both coupling methods lead to variation in the orientation of proteins on the surface and therefore to a distribution of energy barriers, which justifies the application of the DEB model. Consequently, the previously obtained dissociation curves were also fitted by Equation 6, using a typical distance to the transition state of x_β = 0.5 nm and attempt frequency of ω_0 = 3 $\times 10^7$ s^{-1}, which are assumed typical for the kinetics of unbinding governed by viscous friction [16] (**Figure 4**).

As it can be seen in Figure 4, the dissociation curves of Ara h 1 protein–anti-Ara h 1 antibody interaction seem to be explained reasonably well by assuming a DEB model. The obtained fitted parameters were E_0 = 26 ± 1 k_BT and σ = 4.5 ± 1.1 k_BT. Both parameters do not show a trend and are within error bars independent of the applied force (**Figure 5**), confirming the applicability of the model.

Inherent to a distribution of energy barriers originating from molecular inhomogeneity, it is not possible to define a single value for k_{off} (0). However, by using Equation 1, an equivalent k_{off} (0) can be estimated, assuming $\omega_0 = 3 \times 10^7$ s^{-1} as before. The peak of the energy barrier value (26 k_BT) then corresponds to a dissociation rate constant, $k_{off} = 1.5 \times 10^{-4}$ s^{-1}. Since the energy barrier is in the exponent of the rate constant, the most probable k_{off} typically spans a range between 4.2×10^{-4} and 5.6×10^{-5} s^{-1}.

3.4 Inverted configuration of the molecular system: Ara h 1 protein coupled to magnetic particles and anti-Ara h 1 antibody immobilised on substrate

In order to study whether immobilisation of the biomolecules on the polystyrene surface or on the magnetic particles is affecting the affinity of the protein-antibody complex, dissociation experiments with an inverted arrangement of the biomolecules were also performed. In these experiments anti-Ara h 1 antibody was immobilised on the polystyrene surface while Ara h 1 protein was coupled to the magnetic particles. The concentration of antibody on the polystyrene slides was 4 nM (Figure S3). Adsorption of magnetic particles to a polystyrene control slide (coated only with 1% BSA) was not observed in this experimental design either (Figure S3A), proving again that binding of magnetic particles to the polystyrene surfaces is due to the specific interactions between antibody and its protein.

By applying the same range of magnetic pulling forces to the bound particles, from 10 to 40 pN, dissociation curves were obtained. Subsequently, the applicability of the DEB model to these data was tested. Dissociation curves were fitted by Equation 6 assuming the same values as in previous case for ω_0 and x_β (Figure S4). The fitted parameters (**Figure 6**) were $E_0 = 28 \pm 1$ k_BT and $\sigma = 4 \pm 1$ k_BT. Also in this case, they were independent of the applied force, which confirms the applicability of the DEB for this biomolecular configuration (antibody on

particles, protein on substrate). The peak of the central energy barrier value (28 k_BT) corresponds to $k_{off} = 2.1 \times 10^{-5}$ s^{-1}, in the range given by the error in the most probable k_{off}, $5.6 \times 10^{-5} - 7.6 \times 10^{-6}$ s^{-1}.

3.5 Comparison of the dissociation parameters found for the different molecular configurations

When the dissociation rate constants estimated by the DEB model for the two different molecular configurations are compared, it can be seen that for both cases the estimated dissociation rate constant varies within a wide range, of approximately one order of magnitude. This is not only due to molecular inhomogeneities present in the sample but also caused by the introduction of a variation in the measured energy barriers by the magnetic force-induced dissociation experiments themselves. In this type of experiments at least three contributions can lead to a wide distribution of energy barriers. At first, force-induced assays introduce a directionality during dissociation, which is absent in a thermally-based dissociation. The direction of the force is not necessarily along the most favorable path during thermal dissociation which is usually described as the reaction coordinate. Consequently, the variation in the angular distribution between the orientation of the ligand-receptor pair and the direction of the applied force introduces a widening of the energy barrier distribution. A second possible interference involves the interaction of the particle with the surface, which can depend on the local molecular inhomogeneity both on the surface and the particle. A third source of widening the measured distribution is the variation of magnetic content from particle to particle, which translates into a variation in the applied force.

It is also noteworthy that, despite of this wide distribution, the dissociation rate constants corresponding to the peak of the energy barrier distribution estimated for the two different molecular configurations are different by approximately one order of magnitude: $k_{off} \approx 1.5$

$\times 10^{-4}$ s^{-1}, for the configuration with Ara h 1 protein immobilised on the substrate, and $k_{off} \approx 2 \times 10^{-5}$ s^{-1}, for the one with anti-Ara h 1 antibody on the surface. This indicates that the immobilisation of at least one of the biomolecules on the assay surface, namely polystyrene substrate and/or magnetic particles, is affecting the binding affinity of this antibody-protein complex. In the first case the dissociation rate constant is about one order of magnitude bigger, meaning that the measured affinity is lower when the anti-Ara h 1 antibody is immobilised on the surface of magnetic particles and the Ara h 1 protein is physically adsorbed on polystyrene slides than when they are arranged in the inverted configuration. There are two possible explanations for this observation: (1) either the anti-Ara h 1 antibody is more affected by heterobifunctional crosslinking with EDC/NHS chemistry than the Ara h 1 protein is, or (2) the Ara h 1 protein is more disturbed by physisorption than the anti-Ara h1 antibody is. The Ara h 1 protein has a very stable homotrimeric structure [31] and in each of the three monomers there is an epitope for binding with anti-Ara h 1 antibody. Therefore, in the case of immobilisation via EDC/NHS chemistry, even if the protein is captured via amine groups close to one of the epitopes, most likely one of the other two would still be available for binding with the antibody. On the contrary, since only the Fab region of the anti-Ara h 1 antibody binds to the protein, interference with detection capability is more probable if the antibody is captured via amine groups of or adjacent to the protein binding site [32]. Moreover, it has already been described that randomly immobilised antibodies through primary amines will result in a population of immobilised antibodies with no or decreased antigen-binding activity [33]. Regarding immobilisation through physisorption on a substrate, it is known that this approach leads to a mixture of biomolecular orientations [30]. Therefore, passively adsorbed antibodies are not strictly "fab-up" oriented. Moreover, molecular simulations suggest that they are preferentially laying down in a "flat-on" configuration [34]. However it is again highly probable that the Ara h 1 protein has at least one of the three

epitopes optimally oriented, even when being physically adsorbed on a substrate. Taking all of this into consideration, it is hypothesised that the reason why a higher dissociation rate constant is found for the molecular configuration in which the antibody is coupled to the magnetic particles and the protein is adsorbed on the polystyrene substrate, is that the functionality of anti-Ara h 1 antibody is more disturbed than the one of Ara h 1 protein by crosslinking with EDC/NHS.

3.6 Dissociation experiments with surface plasmon resonance (SPR)

In order to explore this further, dissociation experiments for both molecular configurations were also performed with SPR, considered to be a reference technique for quantification and characterisation of biomolecular interactions [17]. It is based on the measurement of the refractive index changes near a sensor surface. In this work, the dissociation rate constant for the Ara h 1–anti-Ara h 1 antibody complex was measured using a Biacore^{TM} instrument. In the first experiment the gold surface of the sensor chip was functionalised with anti-Ara h 1 antibody, while Ara h 1 protein was free in solution. Subsequently the biomolecular configuration was also inverted and therefore Ara h 1 protein was coupled to the chip sensor surface while anti-Ara h 1 antibody was free in solution. The dissociation constants obtained were respectively $k_{off} = 4.2(\pm0.5)x10^{-4}$ s^{-1} and $k_{off} = 3.4(\pm1.7)x10^{-5}$ s^{-1}. The obtained kinetic curves, fitted to a 1:1 Langmuir model, can be found in the Supplementary Information (Figure S5).

The fact that both experimental techniques, force-induced dissociation with MT and SPR, are based on different physical principles and rely on different type of substrates onto which molecules are immobilised, challenges the direct comparison of the dissociation parameters obtained with each of them. Nevertheless, the extracted dissociation rate constants by both

techniques are within the same range (10^{-4}–10^{-5} s^{-1}) and, furthermore, the SPR experiments also provide different dissociation rate constants for both molecular configurations. In this case, dissociation appeared to be slower for the configuration in which the Ara h 1 protein was immobilised on the surface of the chip instead of the antibody. Since in SPR experiments immobilisation of the molecules on the chip surface was also performed through EDC/NHS chemistry, this observation could be again related to the fact that Ara h 1 protein is less affected by crosslinking to the carboxylated dextran layer on the chip than the anti-Ara h 1 antibody, which would increase the possibility that every molecule has one epitope intact for binding. This could possibly lead to rebinding of eluted antibody to another epitope, especially if the density of the protein coating is high, causing the fact that the dissociation rate constant measured in this case is artificially low [35].

4. Conclusions

In this paper, the interaction between the main peanut allergen, Ara h 1 protein, and its monoclonal antibody, anti-Ara h 1, was studied by magnetic force-induced dissociation experiments. In these experiments the biomolecules were arranged in two different configurations and two different theoretical models were employed to analyze the experimental data. The classical multi-exponential Bell and Evans (MBE) model, which assumes several fractions of particles with single energy barriers for dissociation, was not applicable for this antibody-protein complex since the predicted fractions for different bond populations showed a clear dependency on the applied force. Therefore, a recently introduced distributed energy barrier (DEB) model that describes the variation in dissociation rate constants by a distribution of energy barriers was also employed to analyze the data. This model is an extension of the classical MBE model and reflects the inhomogeneity of the molecular interactions as well as the experimentally-generated variations in the force-induced

dissociation experiments. These variations could for example originate from directionality of the applied force and from particle-to-particle differences. The DEB model properly described the distribution present in the interaction of Ara h 1 protein with anti-Ara h 1 antibody. However, when applying this model, surprisingly different dissociation parameters were found depending on how molecules are arranged in the diverse assay surfaces. The found dissociation rate constant was about one order of magnitude smaller for the molecular configuration in which Ara h 1 protein is the molecule coupled to the surface of magnetic particles and the anti-Ara h 1 antibody was passively adsorbed on polystyrene substrates. We hypothesised that the fact that Ara h 1 protein exhibits a very stable homotrimeric structure, and hence has multiple epitopes for binding with the antibody, may lead to a more robust coupling to the magnetic particles through EDC/NHS than the one of anti-Ara h 1 antibody. Consequently in this case the affinity of the complex would be less affected by the coupling. In addition, SPR experiments were performed in order to further investigate this phenomenon. The found dissociation rate constants in this case also appeared to be different depending on the molecule being immobilised on the chip surface. When Ara h 1 protein was immobilised on the chip surface the dissociation rate constant was smaller, which indicates that, also in this case, Ara h 1 protein was less affected by crosslinking with EDC/NHS than the anti-Ara h 1 antibody, possibly due to its trimeric structure.

In conclusion, we have shown that the recently described DEB model by Kemper et al. can be used to interpret the dissociation data of the Ara h 1 protein–anti-Ara h 1 antibody complex. Also, we have demonstrated that for this complex, depending on how molecules were attached to the sensor surface and whether the antibody or the protein was covalently bound, different dissociation parameters were found, also with SPR experiments. Finally we discussed a few hypotheses for the observed behavior. We note that similar effects might be

observed in other protein-antibody systems, especially if multivalent proteins are involved in the assay.

The results of this work highlight the importance of taking into account inhomogeneities present in biosensor surfaces and/or induced by experimental techniques when studying the interaction processes of biomolecular complexes.

Acknowledgements

This research was financially supported by the European Commission's 7th Framework Programme (FP7/2007-2013) under the Grant Agreement BIOMAX (project n°264737) and the Fund for Scientific Research Flanders – FWO (G.0997.11 and G.0861.14).

Figure Legends

Figure 1. Left: Images of anti-Ara h 1 antibody-coated magnetic particles bound to polystyrene surfaces modified with (A) 1% BSA, (B) control protein, IgE, and (C-E) different concentrations of Ara h 1 protein as recorded by the camera. Right: Number of anti-Ara h 1 antibody coated magnetic particles binding to the different functionalised substrates.

Figure 2. Curves representing dissociation of Ara h 1 functionalised magnetic particles from an anti-Ara h 1 antibody coated surface as a function of time. The curves are averages of two replicas. For each applied pulling force, the curves were fitted using a MBE model with two components (Equation 7).

Figure 3. Dissociation parameters extracted from the dissociation curves of the Ara h 1 protein–anti-Ara h 1 antibody complex, fitted by the MBE model (Equation 7). (A) The fitted single-molecular dissociation rate of Ara h 1–anti-Ara h 1 bonds as a function of the applied

force. $k_{off}^{s}(F)$ is fitted linearly and extrapolated to zero force to obtain the spontaneous dissociation rate constant. (B) Fractional occupancy of specific (black) and non-specific (red) bonds at t=0 as a function of the applied force. Every data point represents an individual experiment.

Figure 4. Curves representing dissociation of Ara h 1 functionalised magnetic particles from an anti-Ara h 1 antibody coated surface as a function of time. The curves are averages of two replicas. For each applied pulling force, the curves were fitted using the DEB model (Equation 6).

Figure 5. Energy barrier values, E_0 (A) and the spread σ (B) as extracted from the fitted curves in Figure 4. Every data point represents an individual experiment.

Figure 6. Energy barrier values, E0 (A) and the spread σ (B) as extracted from the fitted curves in Figure S4. Every data point represents an individual experiment.

References

[1] Evans E. Probing the relation between force-lifetime-and chemistry. Annu Rev Biophys Biomol Struct 2001;30:105–28.

[2] Allison DP, Hinterdorfer P, Han W. Biomolecular force measurements and the atomic force microscope. Curr Opin Biotechnol 2002;13:47–51.

[3] Lee C-K, Wang Y-M, Huang L-S, Lin S. Atomic force microscopy: determination of unbinding force, off rate and energy barrier for protein-ligand interaction. Micron 2007;38:446–61.

[4] Evans E, Ritchie K, Merkel R. Sensitive force technique to probe molecular adhesion and structural linkages at biological interfaces. Biophys J 1995;68:2580–7.

[5] Merkel R, Nassoy P, Leung a, Ritchie K, Evans E. Energy landscapes of receptor-ligand bonds explored with dynamic force spectroscopy. Nature 1999;397:50–3.

[6] Ishijima A, Kojima H, Higuchi H, Harada Y, Funatsu T, Yanagida T. Multiple- and single-molecule analysis of the actomyosin motor by nanometer-piconewton manipulation with a microneedle: unitary steps and forces. Biophys J 1996;70:383–400.

[7] Moffitt JR, Chemla YR, Smith SB, Bustamante C. Recent advances in optical tweezers. Annu Rev Biochem 2008;77:205–28.

[8] Dudko OK. Interactions Using Nanopore Force Spectroscopy Spectroscopy. Encyclopedia of Analytical Chemistry, Ed. R. Meyers. John Wiley & Sons, Ltd; 2009.

[9] Neuman KC, Nagy A. Single-molecule force spectroscopy : optical tweezers , magnetic tweezers and atomic force microscopy. Nature Met 2008;5:491–505.

[10] Danilowicz C, Greenfield D, Prentiss M. Dissociation of ligand-receptor complexes using magnetic tweezers. Anal Chem 2005;77:3023–8.

[11] Jacob A, van Ijzendoorn LJ, de Jong AM, Prins MWJ. Quantification of protein-ligand dissociation kinetics in heterogeneous affinity assays. Anal Chem 2012;84:9287–94.

[12] Pérez-Ruiz E, Kemper M, Spasic D, Gils A, van Ijzendoorn LJ, Lammertyn J, et al. Probing the force-induced dissociation of aptamer-protein complexes. Anal Chem 2014;86:3084–91.

[13] Assi F, Jenks R, Yang J, Love C, Prentiss M. Massively parallel adhesion and reactivity measurements using simple and inexpensive magnetic tweezers. J Appl Phys 2002;92:5584–86.

[14] De Vlaminck I, Dekker C. Recent advances in magnetic tweezers. Annu Rev Biophys 2012;41:453–72.

[15] Bell G. Models for the specific adhesion of cells to cells. Science 1978;200:618–27.

[16] Kemper M. Non-specific protein-surface interactions in the context of particle based biosensors. Eindhoven University of Technology, 2013.

[17] Gopinath SCB. Biosensing applications of surface plasmon resonance-based Biacore technology. Sensors Actuators B Chem 2010;150:722–33.

[18] Kleber-Janke T, Crameri R, Appenzeller U, Schlaak M, Becker WM. Selective cloning of peanut allergens, including profilin and 2S albumins, by phage display technology. Int Arch Allergy Immunol 1999;119:265–74.

[19] Lehmann K, Hoffmann S, Neudecker P, Suhr M, Becker W-M, Rösch P. High-yield expression in Escherichia coli, purification, and characterisation of properly folded major peanut allergen Ara h 2. Protein Expr Purif 2003;31:250–9.

[20] Van Hengel AJ. Food allergen detection methods and the challenge to protect food-allergic consumers. Anal Bioanal Chem 2007;389:111–8.

[21] Chang AS, Sreedharan A, Schneider KR. Peanut and peanut products: A food safety perspective. Food Control 2013;32:296–303.

[22] Taylor P, Mills ENC, Potts A, Plumb GW, Lambert N, Morgan MRA. Food and Agricultural Immunology Development of a rapid dipstick immunoassay for the detection of peanut contamination of food. Food Agric Immunol, 1997;9:1, 37-50.

[23] Pomes A, Vinton R, Chapman MD. Peanut Allergen (Ara h 1) Detection in Foods Containing Chocolate. J Food Protect 2004;67:793–8.

[24] Wen H-W, Borejsza-Wysocki W, DeCory TR, Durst R a. Development of a competitive liposome-based lateral flow assay for the rapid detection of the allergenic peanut protein Ara h1. Anal Bioanal Chem 2005;382:1217–26.

[25] Huang Y, Bell MC, Suni II. Impedance Biosensor for Peanut Protein Ara h 1 Impedance Biosensor for Peanut Protein Ara h 1. Anal Chem 2008;80:9157–61.

[26] Pollet J, Delport F, Janssen KPF, Tran DT, Wouters J, Verbiest T, et al. Fast and accurate peanut allergen detection with nanobead enhanced optical fiber SPR biosensor. Talanta 2011;83:1436–41.

[27] Greg T. Hermanson. Bioconjugate techniques. 3rd Edition. Elsevier; 2013.

[28] Myszka DG. Improving biosensor analysis, J Mol Recognit 1999;12:279–84.

[29] Tajima N, Takai M, Ishihara K. Significance of antibody orientation unraveled: well-oriented antibodies recorded high binding affinity. Anal Chem 2011;83:1969–76.

[30] Wiseman ME, Frank CW. Antibody adsorption and orientation on hydrophobic surfaces. Langmuir 2012;28:1765–74.

[31] Maleki SJ, Kopper RA, Shin DS, Park C-W, Compadre CM, Sampson H, et al. Structure of the Major Peanut Allergen Ara h 1 May Protect IgE-Binding Epitopes from Degradation. J Immunol 2000;164:5844–9.

[32] Vashist SK, Dixit CK, MacCraith BD, O'Kennedy R. Effect of antibody immobilisation strategies on the analytical performance of a surface plasmon resonance-based immunoassay. Analyst 2011;136:4431–6.

[33] Podlaski FJ, Stern AS. Site-specific immobilisation of antibodies to protein G-derivatised solid supports. Methods Mol Biol 2000;147:41–8.

[34] Zhou J, Chen S, Jiang S. Orientation of Adsorbed Antibodies on Charged Surfaces by Computer Simulation Based on a United-Residue Model. Langmuir 2003;19:3472–8.

[35] Nieba L, Krebber A, Plückthun A. Competition BIAcore for Measuring True Affinities : Large Differences from Values Determined from Binding Kinetics. Anal Biochem 1996;165:155–65.

Figure 1

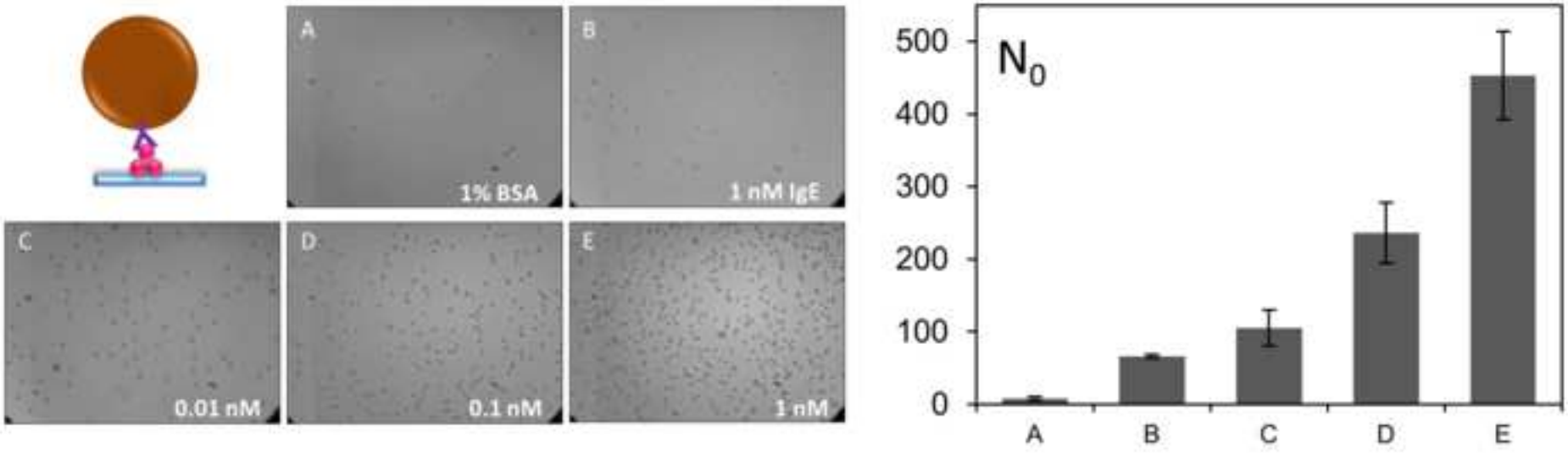

Figure 2

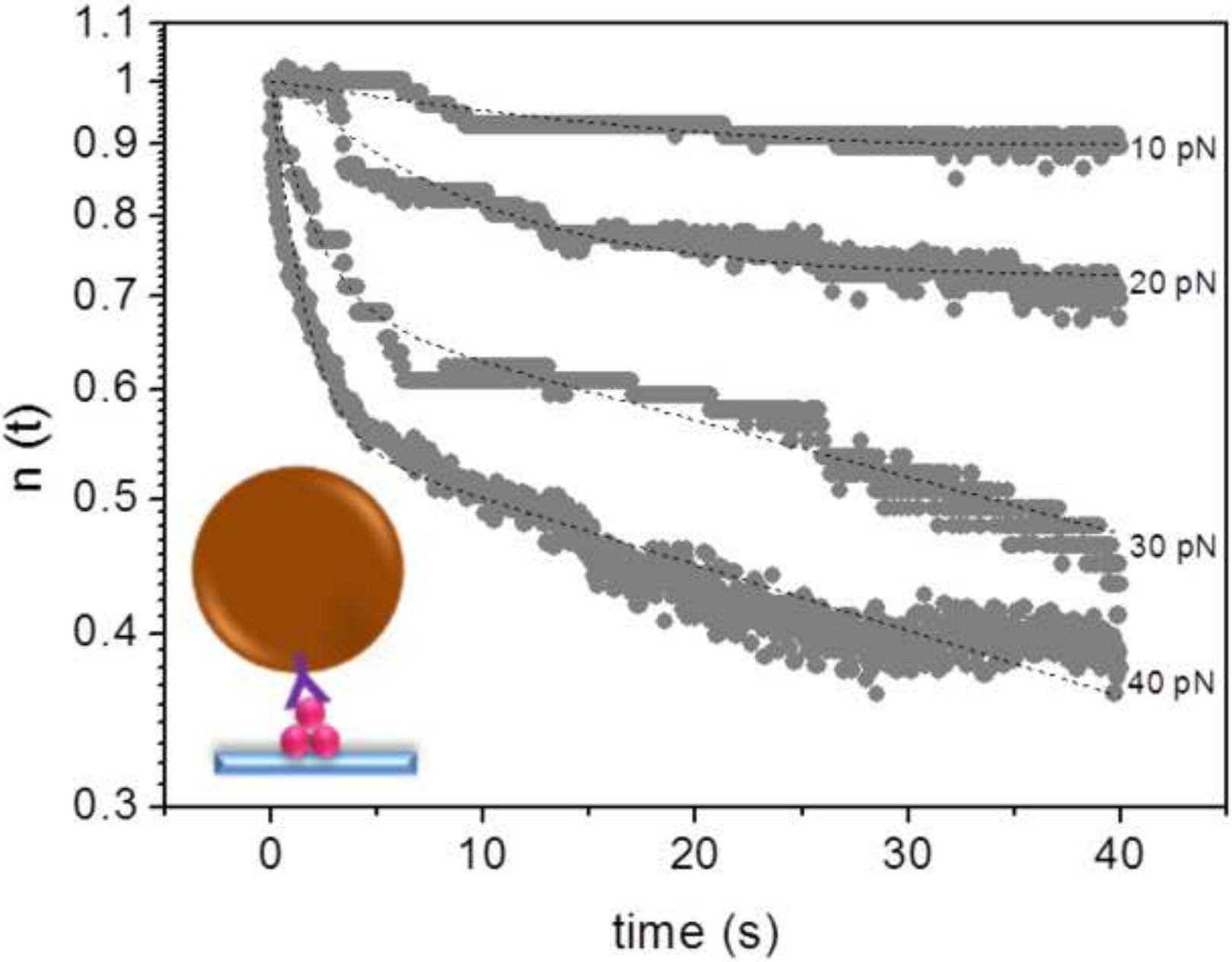

Figure 3

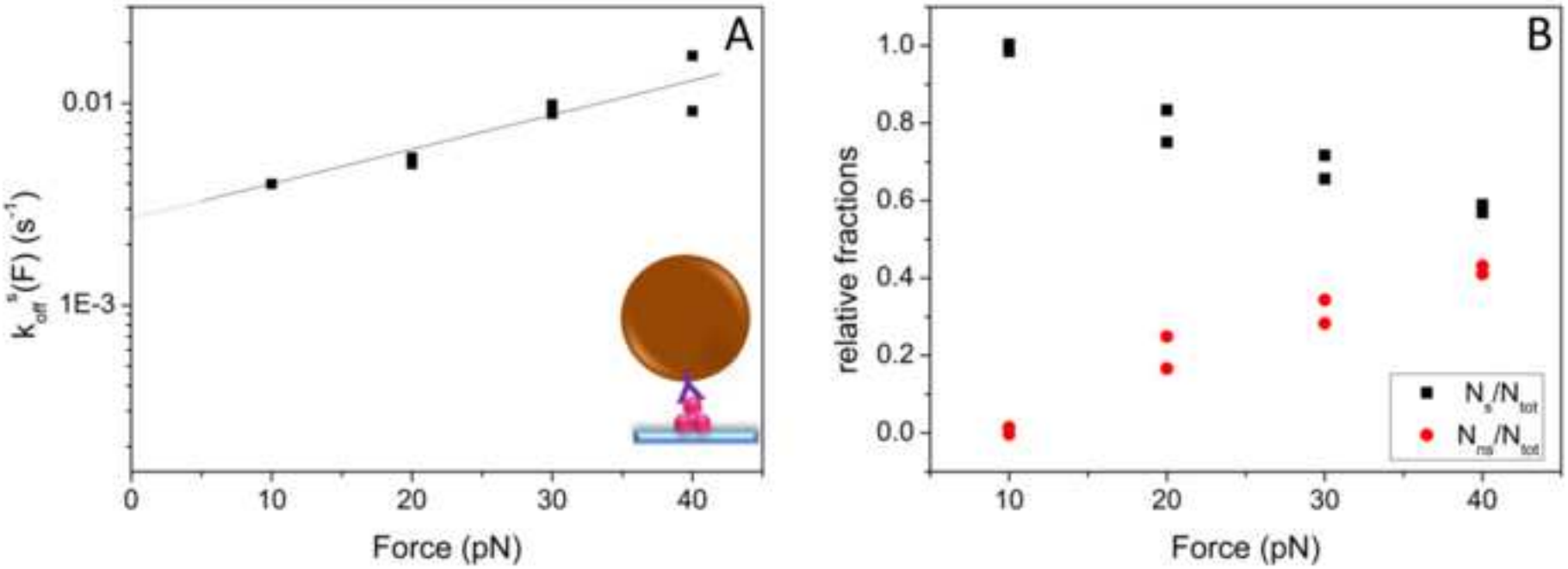
A
0.01
1E-3
$k_{off}^{s}(F)$ (s^{-1})
0
10
20
30
40
Force (pN)
B
1.0
0.8
0.6
0.4
0.2
0.0
relative fractions
N_s/N_{tot}
N_{ns}/N_{tot}
10
20
30
40
Force (pN)

Figure 4

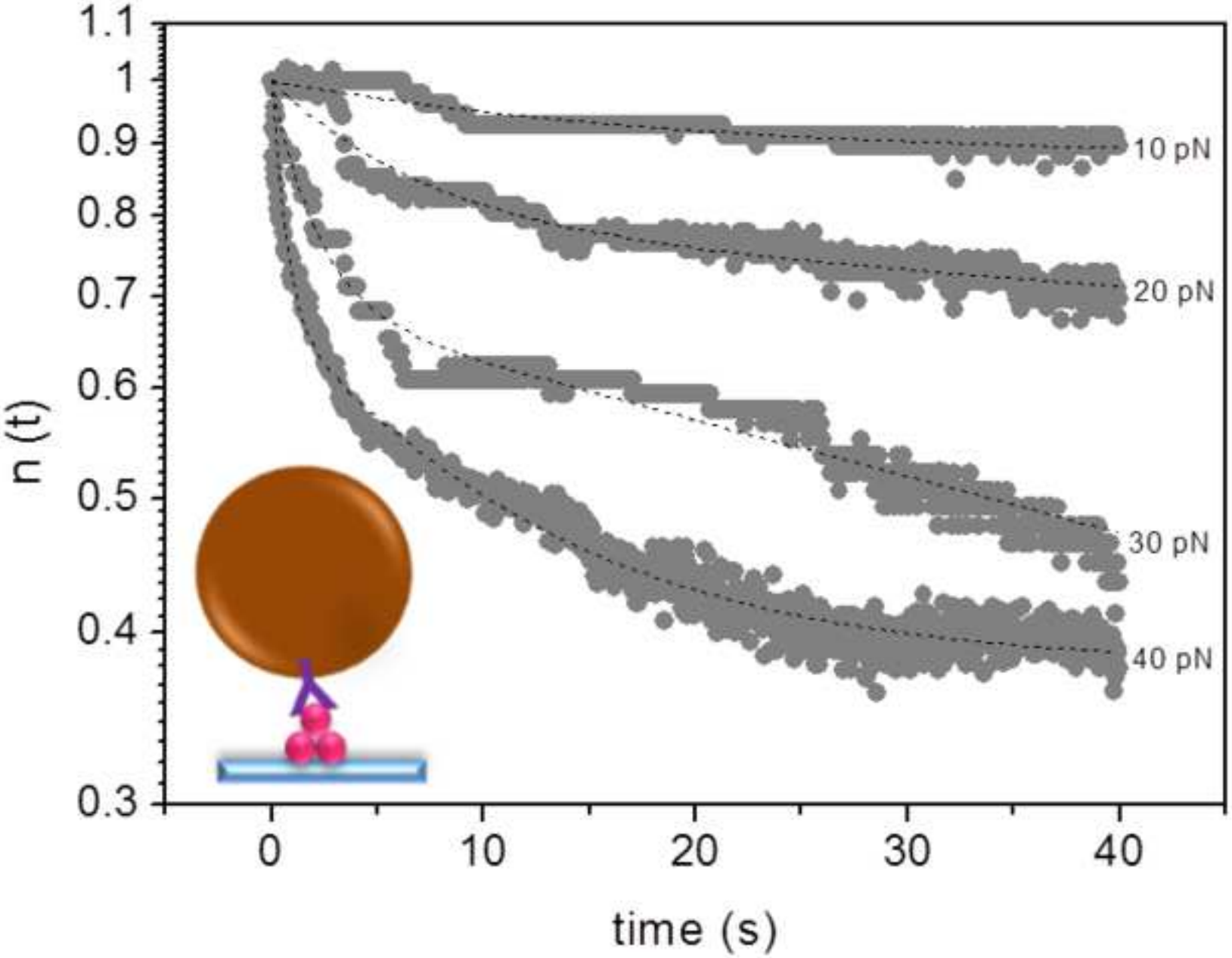

Figure 5

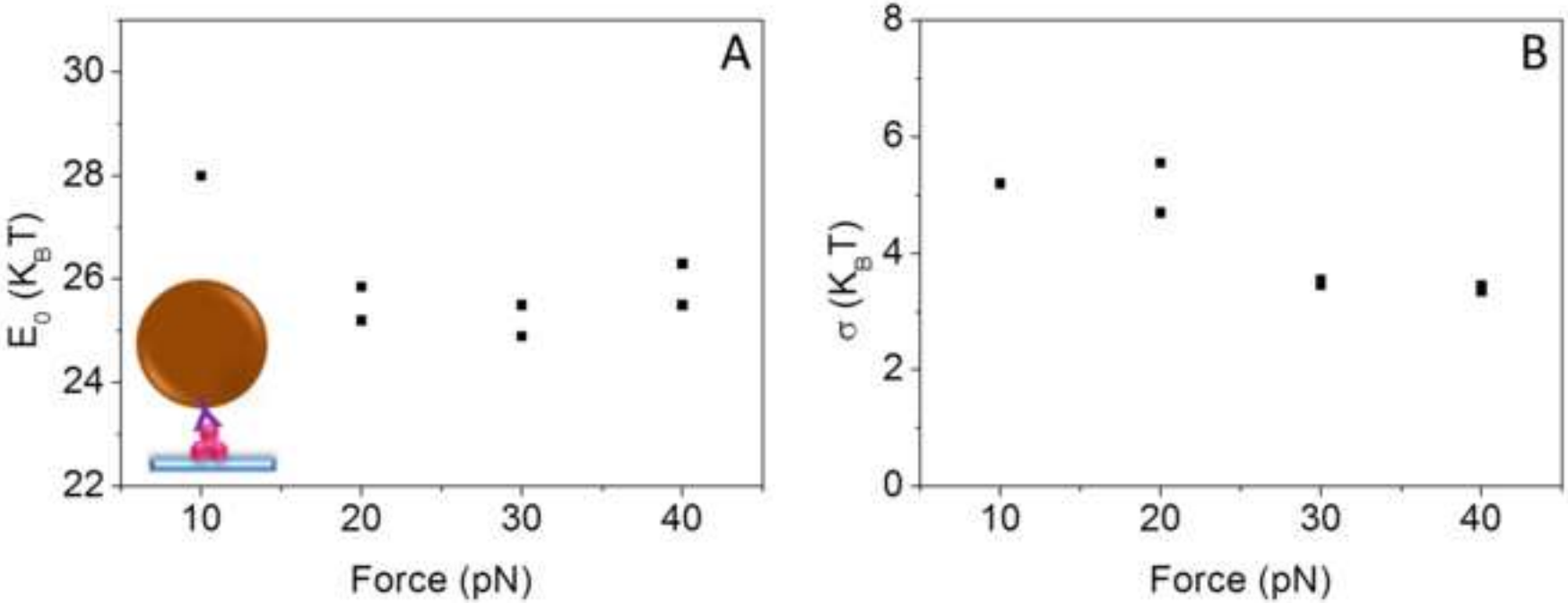

Figure 6

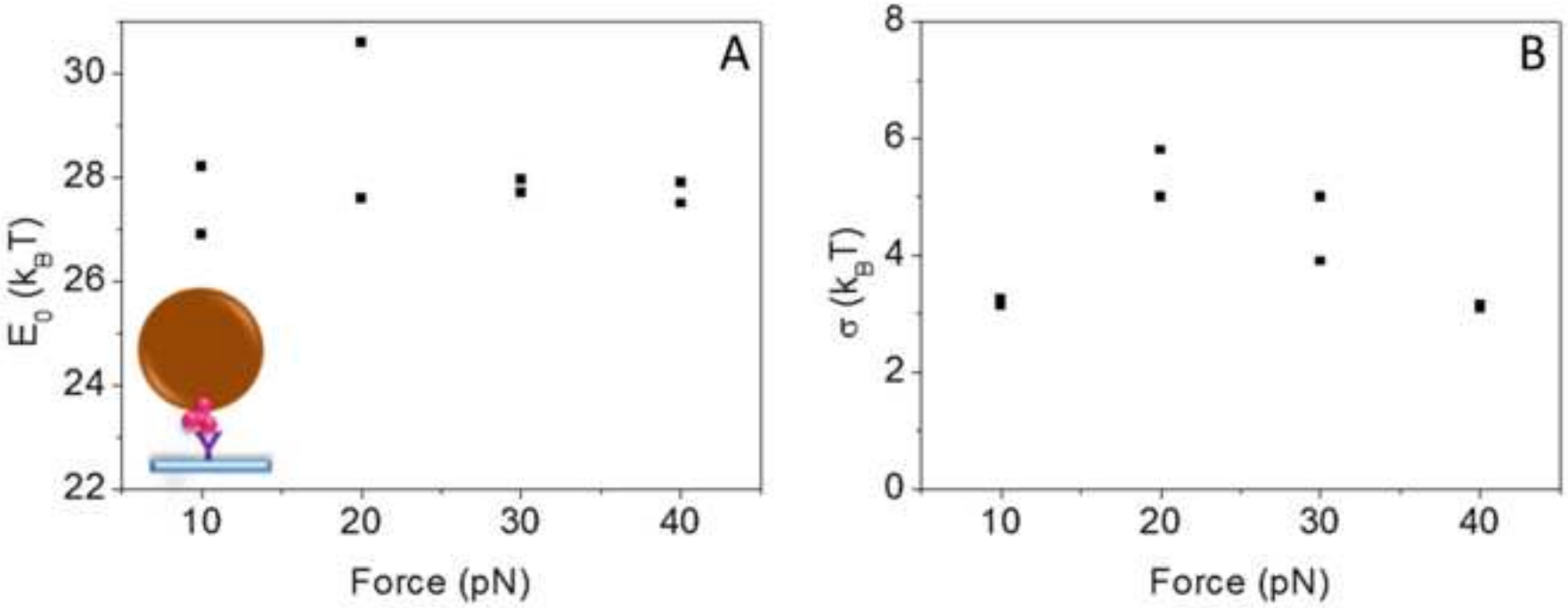
A
B
E_0 (k_BT)
σ (k_BT)
Force (pN)
Force (pN)
22
24
26
28
30
0
2
4
6
8
10
20
30
40